Crystallization behavior of monoglyceride oleogels: a comparison between a fully hydrogenated palm oil and a fully hydrogenated rapeseed oil based monoglycerides

Kato Rondou[1], Fien De Witte[1], Ivana A. Penagos[1,2], Oscar Chen[1], Koen Dewettinck[1,2], Filip Van Bockstaele[1,2]

[1] Food Structure and Function (FSF) Research Group, Department of Food Technology, Safety and Health, Faculty of Bioscience Engineering, Ghent University, Ghent, Belgium

[2] Vandemoortele Centre 'Lipid Science and Technology', Faculty of Bioscience Engineering, Ghent University, Ghent, Belgium

ABSTRACT

Fat polymorphism plays a crucial role in many fat-rich food products (e.g., margarine, chocolate). Due to this, polymorphism of triglycerides is widely investigated. During the previous years, the interest of using monoglyceride oleogels to replace margarine is increasing due to its structure, reduced amount of saturated fatty acids, stability and application potential. However, polymorphism of monoglyceride oleogels is less investigated. This research shows the effect of the composition (C18:0 or C18:0 and C16:0), temperature (25-20-10°C) and production process (static or lab-scale scraped surface heat exchanger) on the crystallization behavior of monoglyceride oleogels (MO) by using differential scanning calorimetry, (synchrotron) X-ray scattering and polarized light microscopy. Based on time-resolved synchrotron WAXS, it was found that the rapeseed oil based MO (MO-C18) occurred in four different polymorphs. During crystallization, transitions from an inverse lamellar phase (Lα) towards sub-α1 and sub-α2 could be established. Upon storage, a polymorphic transition towards β occurred. For the palm oil based MO (MO-C18/C16), only two polymorphs were found during crystallization (Lα, sub-α), followed by a polymorphic transition to β upon storage. By applying high shear and cooling rates during the production of MO-C18 (dynamic production), the polymorphic transition from sub-α2 to β occurred much faster compared to the static production method. When comparing the dynamically produced MO-C18 and MO-C18/C16, the thickness of 1 lamella, the crystal nanoplatelet and the fat crystals were smaller for MO-C18/C16. This research clearly illustrates that the composition and the applied crystallization conditions have an impact on the properties from nano-to microscale.

KEYWORDS: Monoglycerides, crystallization, synchrotron X-ray scattering, lab-scale scraped surface heat exchanger, BWA method, differential scanning calorimetry

GRAPHICAL ABSTRACT

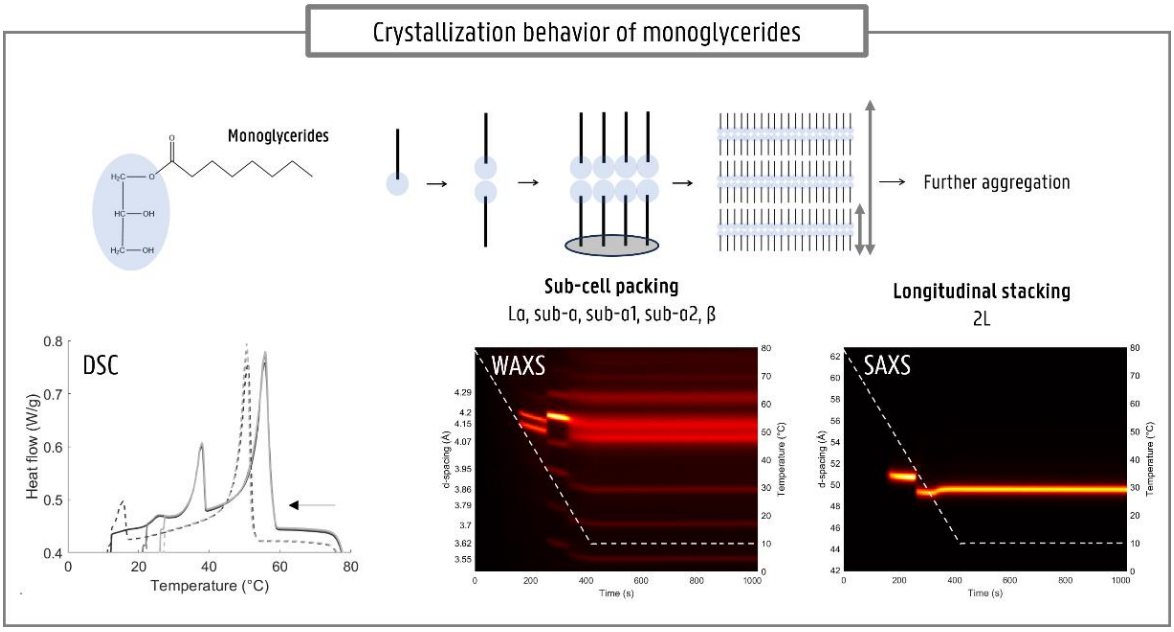

Time-resolved synchrotron SAXS and WAXS together with DSC analysis showed clear differences in the crystallization behavior of two monoglyceride oleogels originating from fully hydrogenated rapeseed oil and fully hydrogenated palm oil (MO-C18 and MO-C18/C16).

PRACTICAL APPLICATIONS

This research illustrates the importance of engineering monoglycerides oleogels to obtain food products with an improved nutritional balance. Hereby, the manuscript focusses on the crystallization behavior of monoglyceride oleogels by changing the composition and the crystallization procedure. The acquired insights go beyond the state of the art. It was found that applying high cooling rates and high shear rates by using a lab-scale scraped surface heat exchanger affected the crystallization behavior of monoglyceride oleogels. These are crucial experiments to verify the application potential of monoglyceride oleogels in the food industry. Moreover, different polymorphic transitions occurred for the two types of monoglycerides. This is the starting point to investigate the effect of polymorphism on a final food product in order to improve the nutritional balance in fat-rich food products.

Funding sources: This work was supported by BOF-UGent (BOF/STA/202009/049), the FWO (Fonds Wetenschappelijk Onderzoek): [Hercules Grant AUGE/17/29], [DUBBLE - ESRF TRAVEL] and Vandemoortele Lipids NV.

Author contributions: Kato Rondou: Investigation, Formal analysis, Visualization, Writing – original draft; Fien De Witte: Investigation, Methodology, Writing – review & editing; Ivana Penagos: Investigation, Methodology, Writing – review & editing; Oscar Chen: Investigation, Writing – review & editing; Koen Dewettinck: Supervision, funding acquisition, resources; Filip Van Bockstaele: Conceptualization, supervision, funding acquisition, Writing – review & editing.

Data availability statement: The dataset used in this manuscript is available in Zenodo at https://doi.org/10.5281/zenodo.10077833.

Conflicts of Interest: The authors declare no conflict of interest.

1 Introduction

Over the years, research has proven that the intake of saturated fatty acids is associated with an increased risk for developing cardiovascular diseases (Forouhi et al., 2018; Nettleton et al., 2017). As a result, the guidelines of the world health organization restrict the intake of saturated fatty acids to maximum 10% of the total energy intake (WHO, 2023). Nonetheless, conventional solid-like fats such as butter and margarine are rich in saturated fatty acids. When applying butter or margarine in bakery products, the saturated fatty acids will largely contribute the final structure and mouthfeel. Simple replacement by oils, high in unsaturated fatty acids, will therefore negatively affect the functionality of the fat in bakery applications. To tackle this, alternative oil structuring routes are investigated to formulate alternatives for butter and margarine in bakery applications. The main goal is to find alternatives with a reduced amount of saturated fatty acids while matching its functionality. A promising approach is oleogelation where gelators (e.g., monoglycerides) can be directly dissolved in oil (direct method) (Patel & Dewettinck, 2016). For monoglyceride oleogels, the crystal network is then formed by the crystallized monoglycerides that are able to entrap a high amount of liquid oil. It is known that monoglycerides can already form a stable network at a concentration of only 4% (Giacomozzi et al., 2018).

The nanoscale properties of fat crystals are typically investigated with X-ray scattering techniques (Walstra, 2001). Hereby, the sub-cell packing is investigated with wide-angle X-ray scattering (WAXS) and the longitudinal stacking with small-angle X-ray scattering (SAXS). Especially time-resolved WAXS and SAXS can be used to gain an in-depth understanding of the crystallization behavior of monoglycerides in oil. Upon cooling below its gelation temperature, the monoglycerides will form an inverse lamellar phase (Lα). Further cooling allows the monoglycerides to transform into the crystalline sub-α polymorph (Chen & Terentjev, 2018). Depending on the composition of the monoglycerides, other polymorphs were found. For monostearin, a distinction can be made between sub-α1 and sub-α2 (Vereecken et al., 2009). Upon longer storage times, the most stable β polymorph will be formed (Lutton, 1971).

Although general insights in the polymorphism of monoglycerides are already described, detailed information is still lacking. Until now, insights in the polymorphism of monoglycerides are limited to the so-called "statically crystallized oleogels", which denotes systems cooled in the absence of shear. However, at industrial level, scraped surface heat exchangers are used to apply high shear rates and high cooling rates during crystallization of shortenings and margarines. The resulting products are referred to as “dynamically crystallized”. This paper includes both statically and dynamically crystallized oleogels to investigate the crystal properties of monoglycerides in oil. First, the effect of the fatty acid composition and the crystallization temperature on the polymorphism of monoglyceride oleogels was investigated by using time-resolved synchrotron SAXS and WAXS. A distinction was made between a fully hydrogenated rapeseed oil based monoglyceride (rich in C18; M-C18) and a fully hydrogenated palm oil based monoglyceride (rich in C18:0 and C16:0; M-C18/C16), cooled till three different temperatures (10-20-25°C). Second, the effect of applying high shear and cooling rates during the production of monoglyceride oleogels was investigated. This was done by using a lab-scale scraped surface heat exchanger. Finally, the thickness of the crystal nanoplatelet (CNP) was obtained from the SAXS profiles utilizing two distinct methods. First, the Scherrer equation was utilized to obtain an average thickness. In addition, the BWA method was applied to account for the heterogeneity of the crystals. All this combined results in a better understanding of the crystallization behavior of monoglyceride oleogels.

2 Materials and methods

2.1 Samples

2.1.1 Monoglycerides

Two commercially available food-grade monoglycerides (M-C18 and M-C18/16) were kindly provided by Vandemoortele (Belgium). M-C18 (MAG purity of 97.3% w/w) originated from fully hydrogenated rapeseed oil, containing mainly C18:0 (90.5% w/w). M-C18/16 (MAG purity of 96.4% w/w) originated from fully hydrogenated palm oil and is rich in C18:0 (53.6% w/w) and C16:0 (43.1% w/w).

2.1.2 Monoglyceride oleogels

Rapeseed oil was purchased from Ranson (Belgium). Monoglyceride oleogels were made by adding M-C18 and M-C18/C16 to rapeseed oil in a concentration of 10% (w/w). This mixture was heated till 80°C while stirring to obtain a homogeneous solution. The crystallization step was done using two different approaches, namely statically and dynamically. For the statically crystallized oleogels, the homogeneous solution was poured into 125 mL containers and cooled in a freezer at -16°C until the oleogel reached a temperature of 20°C. The dynamic production was performed by using a lab-scale scraped surface heat exchanger (Het Stempel; Zwijndrecht, The Netherlands) in which the sample with an inlet temperature of 80°C was pumped through a scraped surface heat exchanger operating at 1000 rpm with a pump speed of 20 rpm. The flow rate was 43.4-46.4 g/min, resulting in an outlet temperature of 11-13.5°C. Both the statically and dynamically crystallized oleogels were stored at 20°C and will respectively be referred to as StMO and DyMO.

2.2 Differential scanning calorimetry

The crystallization behavior of the monoglycerides and the monoglyceride oleogels was investigated by differential scanning calorimetry (DSC; Q1000—TA instruments). The sample (5-10 mg) was added to aluminium DSC pans. For M-C18 and M-C18/C16, the sample was heated till 100°C for 10 min after which a cooling ramp at 10°C/min till 0°C was applied. For StMO-C18 and StMO-C18/C16, the sample was heated till 80°C for 10 min, followed by a cooling step at 10°C/min to a final crystallization temperature and an isothermal crystallization time of 10 min. This procedure was repeated for different crystallization temperatures (10, 20, 25°C). The onset temperature of crystallization was calculated in Universal Analysis 2000 (TA instruments).

2.3 X-ray scattering

2.3.1 Synchrotron SAXS and WAXS

Simultaneous SAXS and WAXS measurements were performed at the DUBBLE beamline BM26 at the European Synchrotron Radiation Facility (ESRF; Grenoble, France). The X-rays with a wavelength of 1.033 Å at 12 keV were generated in a 16 bunch mode. The SAXS patterns were collected by using a Pilatus 1M detector and WAXS with a 300K-W linear Pilatus detector. For the time-resolved measurements, a small amount of sample was added in a 1 mm quartzglass capillary and heated till 80°C for 10 min prior to the analysis. The same heating-cooling protocol as the DSC measurements was applied. The temperature was controlled with a Linkam stage (THMS600). The acquisition time was 3 s and the SAXS and WAXS spectra were corrected by subtracting the intensity of an empty capillary. The time-resolved SAXS and WAXS are here presented with a heatmap. For the single measurements, a small amount of dynamically crystallized oleogel was added between two layers of Kapton tape and the temperature was kept at 20°C. The

acquisition time was 10 s and the spectra were corrected for the two layers of Kapton. The abbreviation 'SR-' is used to indicate synchrotron data.

2.3.2 Lab-scale SAXS and WAXS

The polymorphism of the statically and dynamically produced samples as function of the storage time was analyzed with a Xeuss 3.0 XRS system (Xenocs; Grenoble, France) operating with an Eiger2R 1M detector (Dectris). The X-ray beam was generated by a Cu-source (Genix 3D) with a wavelength of 1.54 Å at 50 kV and 0.60 mA. The sample-to-detector distance for WAXS and SAXS was respectively 55 mm and 360 mm with an acquisition time of 60 s and 600 s. The oleogels were spooned between two layers of Kapton tape and the temperature was kept at 20°C by using a Peltier system. The intensity was corrected for the scattering of the two layers of Kapton.

2.3.3 Data processing SAXS

The thickness of the average crystal nanoplatelet (CNP) was calculated by using the Scherrer equation $\left(\frac{2\cdot\pi\cdot K}{FWHM}\right)$ in which FWHM is the full width at half maximum and K is the shape factor (K=0.9) (Acevedo & Marangoni, 2010; Langford & Wilson, 1978). Only one replicate was performed. To investigate the heterogeneity of the CNP thickness, the Bertaut-Warren-Averbach (BWA) method was used. Hereby, a volume-weighted distribution of the CNP thickness is calculated after applying a Fourier transformation as described by Rondou et al. (2022).

2.4 Polarized light microscopy

Polarized light microscopy (Leica DM2500, Belgium) was used to visualize the fat crystal network of the oleogels. A small amount of sample was added to the microscope slide and gently covered with the cover slip. The samples were kept at 20°C by using a Linkam cooling system and a x10 magnification (HCX PL Fluotar 10x/0.3) was used. Images were acquired with the Leica Application Suite (LAS) software.

2.5 Statistics

Significant differences between MO-C18 and MO-C18/C16 were analyzed with R studio (version 2023.03.1). First, the Levene and Shapiro-Wilk test were performed to analyze the homogeneity of the variances and the normality. For not normally distributed data, the non-parametric Mann Whitney U test was used. For normally distributed data, the two sample t-test was used for equal variances and the Welch test for unequal variances to compare the means. All tests were performed with a significance level of 0.05.

3 Results and discussion

3.1 Crystallization behavior of M-C18 and M-C18/C16

The crystallization curves of the neat monoglycerides are shown in Figure 1. Furthermore, the onset and peak temperature of crystallization is summarized in supplementary data (Table S1). Upon cooling, it can be observed that M-C18 starts to crystallize at a higher temperature (around 72°C) compared to M-C18/C16 (around 68°C). For M-C18, three exothermic peaks could be distinguished around 68°C, 33°C and 18°C. Contrarily, M-C18/C16 showed only two exothermic peaks at 65°C and 13°C. These differences are linked to their composition where M-C18 is rich in monostearin while M-C18/C16 is rich in both monostearin and monopalmitin. The crystallization behavior of monostearin was investigated by Vereecken et al. (2009) where the presence of three crystallization peaks was also found. The first peak corresponds to the formation of an inverse lamellar phase (Lα), while the other two correspond respectively to the sub-α1 and sub-α2 polymorph (Vereecken et al., 2009). Verstringe et al. (2013) analyzed the crystallization behavior of monopalmitin. It was found that monopalmitin showed two crystallization peaks, corresponding to the formation of the Lα polymorph and the sub-α polymorph. For M-C18/C16, the same crystallization behavior was found, although the monopalmitin content was only 43.1%. This was also obtained by Lopez-Martinez et al. (2014) by analyzing a commercial monoglyceride containing monopalmitin and monostearin. They report that the transition from sub-α1 to sub-α2 only occurs for fatty acids with a chain length equal or higher than 18 carbon atoms and that the transition is sensitive to the presence of impurities (López-Martínez et al., 2014; Lutton, 1971). Therefore, it is concluded that the high concentration of monopalmitin will most likely hinder the formation of the sub-α2 polymorph in M-C18/ C16.

3.2 Crystallization behavior of MO-C18 and MO-C18/C16

3.2.1 Effect of composition

Monoglyceride (10%) oleogels were made by adding rapeseed oil to the monoglyceride. Hereby, the monoglycerides were diluted, which resulted in a shift for the crystallization onset temperature towards lower temperatures (Figure 2, Table S1). For the onset temperature of the polymorphic transition, this shift was less pronounced. Upon cooling of MO-C18, the transformation of the liquid state to Lα, Lα to sub-α1 and sub-α1 to sub-α2 were initiated respectively at 57.6°C, 38.8°C and 28.5°C (Table 1). For MO-C18/C16, the onset temperature of crystallization occurred at 52.2°C and the polymorphic transition towards sub-α at 15.7° C.

More insight in the different polymorphs formed was obtained with SR-time-resolved WAXS and SAXS. Figure 3 A-C shows the SR-time-resolved WAXS of MO-C18 when cooled at 10°C/min. Similarly to Figure 2, three different phases can be distinguished. Between 80°C and 55°C, no peaks were present due to the liquid state of MO-C18. Starting from 55°C, two peaks with d-spacings 4.20 Å and 4.15 Å appeared. These correspond to the formation of the inverse lamellar phase (Lα). Chen et al. (2008) described similar spacings of 4.17 Å and 4.11 Å for 10% monoglycerides in hazelnut oil (Chen et al., 2008). The small differences can be attributed to the differences in the composition of the oleogels. These spacings are characteristic for the hexagonal packing where 4.20 Å represents the distance between two neighboring glycerol heads within the layer and 4.15 Å the distance between glycerol heads inside the bilayer. There are no peaks related to the fatty acid chain so that the Lα polymorph is not a truly crystalline state as mentioned by Chen et al. (2018). Between 35°C and 20°C, one sharp peak at 4.20 Å, coming from the glycerol heads, and multiple peaks between 3.63 and 4.28 Å appeared. This represents the orthorhombic

packing of the sub-α1 polymorph. Finally, the transformation from sub-α1 to sub-α2 occurred when reaching 20°C. These results are in line with literature (López-Martínez et al., 2014; Vereecken et al., 2009; Watanabe, 1997). The onset temperature of crystallization was always higher than the temperature of the isothermal crystallization (25-20-10°C). Therefore, the differences in the final crystallization temperature during the time-resolved experiments did not have an impact on the polymorphism of MO-C18. This is not the case for MO-C16/C18 where the onset temperature for the α to sub-α transformation was only 16.7°C. This resulted in a different final polymorph when the crystallization process was stopped at 20°C and 25°C compared to 10°C (Figure 3 D-F).

At the start of the crystallization process of MO-C18/C16, the two peaks corresponding to the hexagonal packing of the glycerol heads (Lα) are present around 4.20 Å and 4.15 Å for the three temperatures (Figure 3 D-F). When the crystallization temperature was set at 25°C, no further polymorphic transitions occurred given the too high temperature. When cooling till 20°C, the temperature was low enough to initiate a transition, however, only one sharp peak around 4.20 Å and undefined peaks at lower d-spacings could be observed. When cooling below the onset temperature of the transformation towards to sub-α polymorph, one sharp peak at 4.20 Å and multiple peaks between 4.25 Å and 3.64 Å occurred. When comparing the results of cooling till 20°C and cooling till 10°C, it can be seen that the same d-spacings were found for the packing of the glycerol head (4.20 Å) while there are differences in the crystalline peaks of the fatty acid chains. It might therefore be that at 20°C, the monoglycerides molecules change from an hexagonal packing to an orthorhombic packing without being truly crystalline. This hypothesis is based on the presence of a shift in the d-spacings while clear peaks related to the packing of the fatty acid chains are still missing at 20°C.

Figure 4 A-C shows the SR-time-resolved SAXS profile of MO-C18 in which the formation of the Lα, sub-α1 and sub-α2 polymorph respectively corresponds to long spacings of 50.7, 49.3 and 49.6 Å. The d-spacings of sub-α are smaller compared to the d-spacing of Lα due to the angle of the fatty acid chain, with respect to the lamellar plane, of the orthorhombic packing (Hagemann, 1988). During the formation of the sub-α1 polymorph, the intensity of the Lα peak decreased simultaneously with an increase in the intensity of sub-α1 peak as illustrated in Figure 5B. This indicates a temporary coexistence of Lα and sub-α1. Contrarily, a more gradual shift occurred for the transformation from sub-α1 to sub-α2 (Figure 5C). For MO-C18/C16, the evolution of the SR-SAXS peak is shown in Figure 4 D-F, where a slight decrease from 51.1 Å to 50.1 Å was observed when going from Lα to sub-α. Hereby, this transition occurred gradually without the presence of two peaks at the same time (Figure 5E).

Next to the peak position, the full width at half maximum (FWHM) is commonly analyzed to characterize the thickness of crystal nanoplatelets. In general, the FWHM results from the sum of peak broadening related to the instrument, the microstrain and the crystal thickness (Cullity & Stock, 2014). For synchrotron data, instrumental broadening is reduced compared to lab-scale data. The contribution of micro strain is typically analyzed with the Williamson-Hall plot by using the FWHM of the first and higher order peaks (Cullity & Stock, 2014; Mote et al., 2012). In this paper, the MAG are diluted in liquid oil limiting the construction of the Williamson-Hall plot. In the SAXS region, the signal of the oil can be seen as a 'bump' in the baseline which does not interfere with the first order peak. Contrarily, it overlaps with the higher order peaks, especially the second order peak almost disappears. Since it is not the main interest of this paper to characterize the strain, it is assumed that the contribution of the strain is limited based on preliminary results (synchrotron data of MO-C18 and MO-C18/C16) indicating that the order of magnitude is below 10^{-3}. As a result, it is assumed that the FWHM resembles shifts in crystallite thickness in the

studied systems. The crystal thickness, which is in this case the CNP thickness, is commonly calculated by applying the Scherrer equation (Acevedo & Marangoni, 2010; den Adel et al., 2018; Marangoni et al., 2020). The use of the Scherrer equation is limited to the average size. On the one hand, this limitation is linked to the resolution of the equipment where a maximum size of 100-200 nm is described in literature (Muniz et al., 2016; Rabiei et al., 2020). On the other hand, the limit is based on the diffraction theory. The Scherrer equation has similar assumptions as the ones made for the kinematical theory of X-ray diffraction. This theory is used for small crystals and crystals with defects. As the crystallite size increases and the amount of defects decreases, the kinematical theory looses its accuracy and the dynamical theory is more reliable. In the dynamical theory, the interaction between the incident beam, diffracted beam and all waves inside the crystals are included (Muniz et al., 2016). However, Muniz et al. (2016) demonstrated that the Scherrer equation is still reliable for crystallite sizes up to 600 nm (with allowed error of 20%) when the linear absorption coefficient is less then 2117.3 cm^{-1}. This conclusion was made when comparing the thickness obtained with the Scherrer equation with the one obtained from dynamical models for Si, CeO_2 and LaB_6 crystallites (Muniz et al., 2016). In this part, synchrotron data is used so that it can be assumed that the size limitation is not related to the resolution of the equipment. Nevertheless, the size limit based on the diffraction theory is not known for fat crystals. Therefore, it is assumed that it is be possible to use the Scherrer equation for CNP thicknesses larger than 200 nm, but results should be interpreted carefully. When applying the Scherrer equation to the first order SAXS peak after an isothermal time of 10 minutes at 25, 20 or 10°C (final measurement), the CNP thickness of MO-C18 was between 356 nm and 365 nm and between 316 nm and 333 nm for MO-C18/C16 (Table 2).

3.2.2 Effect of processing

The results obtained from the time-resolved X-ray scattering in the previous part provide information on the static crystallization behavior of the monoglyceride oleogels. However, processing conditions (e.g. shear and cooling rate) have a pronounced effect on crystal networks (Rondou et al., 2022). Therefore, the monoglyceride oleogels were also dynamically produced on a bench-top crystallizer unit. Figure 6 shows the microstructure of the statically and dynamically crystallized samples. The high shear and cooling rate during the dynamic production resulted in the presence of smaller crystals for MO-C18 and MO-C18/C16 compared to the static productions. Within the same production method, smaller crystals were found for MO-C18/C16 compared to MO-C18.

Evaluation of the polymorphism of MO-C18 and MO-C18/C16 as function of the storage time was done by using lab-scale XRS data and visualized in Figure 7. For MO-C18, major differences were found between the WAXS profile of the dynamically (DyMO) and the statically crystallized oleogels (StMO) measured 1 day after the production. For DyMO-C18, one clear peak at 4.58 Å and two smaller ones at 4.0 and 3.82 Å were present which corresponds to the β-polymorph. Nevertheless, StMO-C18 showed one clear peak around 4.15 Å and multiple peaks in 4.32-3.57 Å, corresponding to the sub-α2 polymorph. Starting from one week after the production of StMO-C18, the peak corresponding to the β polymorph around 4.55 Å occurred. After 7 weeks of storage, only the β polymorph remained. This illustrates that the polymorphic transition to the most stable β polymorph is promoted when applying a high shear and cooling rate during the crystallization of MO-C18. In contrast, this was not observed for MO-C18/C16 where both the dynamically and statically crystallized oleogel showed the β polymorph with one clear peak around 4.6 Å and two smaller peaks around 3.93 and 3.75 Å after one day of the production. Subsequently, no further follow-up results are reported. Until now, research about the effect of polymorphism of monoglycerides on the properties of final food applications is only scarcely investigated. The faster transition towards β for

the dynamically produced MO-C18 can be beneficial or to avoid in terms of product quality (stability, mouthfeel, texture, …). The research of Heymans et al. (2018) investigated the foamability of 10% monoglycerides (mainly C16:0 and C18:0) in sunflower oil by applying different cooling protocols. They found that the highest foamability value was found for the samples in which crystallization was not finished (during crystallization in α) and the lowest value for the sample that was crystallized into sub-α. Intermediate values were found for samples crystallized in α and β (Heymans et al., 2018). It is thus possible that polymorphism may impact oleogel functionality, which needs to be further investigated.

In part 3.2.1, it was illustrated that the CNP thickness exceeded 200 nm when using time-resolved synchrotron data. Since this part uses lab-scale data, the resolution of the equipment might be too low to characterize the thicker CNPs, so that these results should be interpreted carefully (see part 3.2.1). For both MO-C18 and MO-C18/C16, the peak of StMO is narrower compared to DyMO, even when both in β (Figure 7, bottom). Since the CNP thickness is inversely related to the full width at half maximum, the number of lamellae within the crystal nanoplatelet of the statically crystallized sample was higher compared to the dynamically crystallized ones. This was also observed by Acevedo and Marangoni (2010) and Mishra et al. (2023) for triglyceride based samples (Acevedo & Marangoni, 2010; Mishra et al., 2023). To the best of our knowledge, the effect of shear on the lamellar thickness of monoglycerides has not yet been reported in literature.

Contrarily to the statically produced samples, the CNP thickness of the dynamically produced samples did not exceed the limit of 200 nm (synchrotron data). A more in-depth analysis of the thickness of the dynamically produced samples was done by applying the BWA method on synchrotron data (SR-DyMO). The BWA method visualizes the heterogeneity of the sample in terms of a volume-weighted frequency distribution (Rondou et al., 2022). These distributions are visualized in Figure 8. It can be seen that the center of the distribution of SR-DyMO-C18 shifts towards the right compared to SR-DyMO-C18/C16, indicating thicker CNPs. This was confirmed by calculating the volume-weighted average number of lamellae per CNP, which was 12.9 and 8.9 for respectively SR-DyMO-C18 and SR-DyMO-C18/C16. Additionally, the thickness of 1 lamella was 49.9 Å for SR-DyMO-C18 and 48.0 Å for SR-DyMO-C18/C16. Hereby, it can be observed that both the thickness of one lamella and the CNP thickness are smaller for SR-DyMO-C18/C16. The presence of C16:0 next to C18:0 might act as an impurity, hindering the longitudinal growth of the of the CNPs. The final microstructure of DyMO-C18/C16 also showed smaller crystals compared to DyMO-C18 as illustrated in Figure 6. The same trend was observed when applying the Scherrer equation (SR-DyMO-C18: 19.4 lamellae, SR-DyMO-C18/C16: 11.4 lamellae). Nevertheless, the thickness of the first order SAXS peak can be influenced by the fatty acid distribution of the hardstocks in which MO-C18 has a higher purity in terms of the fatty acid composition compared to MO-C18/C16.

4 Conclusion

Two different monoglycerides were used to investigate the crystallization behavior of monoglyceride oleogels. MO-C18 originated from fully hydrogenated rapeseed oil, rich in C18:0 (90.5% w/w) and MO-C18/C16 from fully hydrogenated palm oil, rich in C18:0 (53.6% w/w) and C16:0 (43.1% w/w). Time-resolved experiments were performed at the European Synchrotron Radiation Facility to gain an in-depth understanding of the polymorphic transitions of MO-C18 and MO-C18/C16 during crystallization. Time-resolved WAXS showed the presence of three polymorphs for MO-C18 (Lα, sub-α1, sub-α2) and two for MO-C18/C16 (Lα, sub-α). However, when cooling MO-C18/C16 to a temperature slightly higher than the onset temperature of the polymorphic transition towards sub-α, an intermediate form between Lα and

sub-α was found. In addition to the static crystallization (no shear, low cooling rate), a lab-scale scraped surface heat exchanger was used to produce the monoglyceride oleogels (dynamically crystallized). In this way, industrial crystallization processes are simulated, which is essential for gaining insight into their application potential. For both monoglyceride oleogels, statically or dynamically produced, a polymorphic transition towards the most stable β polymorph was found upon storage. Remarkably, the start of the polymorphic transition towards the β polymorph occurred after a storage time of 1 week for the statically produced MO-C18 while it was only 1 day for the other samples. More detailed information about the heterogeneity of the CNP thickness of the dynamically produced monoglyceride oleogels was obtained by applying the BWA method. The distributions calculated with the BWA method showed that the CNPs of MO-C18/C16 contained less and smaller lamellae (8 lamellae; 48.0 Å) compared to MO-C18 (12.9 lamellae; 49.9 Å). This research illustrates the effect of the composition and the crystallization conditions on the crystallization behavior of two monoglyceride oleogels, however, further research is necessary to link these insights to their functionality.

ACKNOWLEDGEMENTS:

We acknowledge the European Synchrotron Radiation Facility (ESRF) for provision of synchrotron radiation facilities under proposal number A26-2-951 at the DUBBLE beamline and we would like to thank Martin Rosenthal for assistance and support in using beamline BM26. The FWO (Fonds Wetenschappelijk Onderzoek) is recognized for its financial support in the acquisition of the Xenocs Xeuss 3.0 X-ray Scattering (XRS) equipment (FWO Hercules Grant AUGE/17/29) and the PhD fellowship of co-authors Fien De Witte (1128923N) and Ivana A. Penagos (1SA5321N). Vandemoortele Lipids NV is acknowledged for providing the monoglycerides and its financial support to the Vandemoortele Centre "Lipid Science and Technology" at Ghent University.

5 References

Acevedo, N. C., & Marangoni, A. G. (2010). Characterization of the Nanoscale in Triacylglycerol Crystal Networks. *Crystal Growth & Design*, *10*(8), 3327-3333. https://doi.org/10.1021/cg100468e

Chen, C.-H., Damme, I., & Terentjev, E. (2008). Phase behavior of C18 monoglyceride in hydrophobic solutions. *Soft Matter*, *5*. https://doi.org/10.1039/B813216J

Chen, C.-H., & Terentjev, E. M. (2018). Chapter 5 - Monoglycerides in Oils. In A. G. Marangoni & N. Garti (Eds.), *Edible Oleogels (Second Edition)* (pp. 103-131). AOCS Press. https://doi.org/https://doi.org/10.1016/B978-0-12-814270-7.00005-8

Cullity, B., & Stock, S. (2014). Elements of X-ray Diffraction. Harlow. In: United Kingdom, Pearson.

den Adel, R., van Malssen, K., van Duynhoven, J., Mykhaylyk, O. O., & Voda, A. (2018). Fat Crystallite Thickness Distribution Based on SAXD Peak Shape Analysis. *European Journal of Lipid Science and Technology*, *120*(9), 1800222. https://doi.org/10.1002/ejlt.201800222

Forouhi, N. G., Krauss, R. M., Taubes, G., & Willett, W. (2018). Dietary fat and cardiometabolic health: evidence, controversies, and consensus for guidance. *BMJ*, *361*, k2139. https://doi.org/10.1136/bmj.k2139

Giacomozzi, A., Carrín, M. E., & Palla, C. A. (2018). Muffins Elaborated with Optimized Monoglycerides Oleogels: From Solid Fat Replacer Obtention to Product Quality Evaluation. *Journal of Food Science*, *83*(6), 1505-1515. https://doi.org/https://doi.org/10.1111/1750-3841.14174

Hagemann, J. (1988). Thermal behavior and polymorphism of acylglycerides. In *Crystallization and polymorphism of fats and fatty acids* (Vol. 31, pp. 9-95). Marcel Dekker New York.

Heymans, R., Tavernier, I., Danthine, S., Rimaux, T., Van der Meeren, P., & Dewettinck, K. (2018). Food-grade monoglyceride oil foams: The effect of tempering on foamability, foam stability and rheological properties. *Food & Function*, *9*. https://doi.org/10.1039/C8FO00536B

Langford, J. I., & Wilson, A. J. C. (1978). Scherrer after sixty years: A survey and some new results in the determination of crystallite size. *Journal of Applied Crystallography*, *11*(2), 102-113. https://doi.org/doi:10.1107/S0021889878012844

López-Martínez, A., Morales-Rueda, J. A., Dibildox-Alvarado, E., Charó-Alonso, M. A., Marangoni, A. G., & Toro-Vazquez, J. F. (2014). Comparing the crystallization and rheological behavior of organogels developed by pure and commercial monoglycerides in vegetable oil. *Food Research International*, *64*, 946-957. https://doi.org/https://doi.org/10.1016/j.foodres.2014.08.029

Lutton, E. S. (1971). The phases of saturated 1-monoglycerides C14-C22. *Journal of the American Oil Chemists' Society*, *48*(12), 778-781. https://doi.org/https://doi.org/10.1007/BF02609279

Marangoni, van Duynhoven, J. P. M., Acevedo, N. C., Nicholson, R. A., & Patel, A. R. (2020). Advances in our understanding of the structure and functionality of edible fats and fat mimetics. *Soft Matter*, *16*(2), 289-306. https://doi.org/10.1039/c9sm01704f

Mishra, K., Kummer, N., Bergfreund, J., Kämpf, F., Bertsch, P., Pauer, R., Nyström, G., Fischer, P., & Windhab, E. J. (2023). Controlling lipid crystallization across multiple length scales by directed shear flow. *Journal of Colloid and Interface Science*, *630*, 731-741. https://doi.org/https://doi.org/10.1016/j.jcis.2022.10.005

Mote, V. D., Purushotham, Y., & Dole, B. N. (2012). Williamson-Hall analysis in estimation of lattice strain in nanometer-sized ZnO particles. *Journal of Theoretical and Applied Physics*, *6*(1), 6. https://doi.org/10.1186/2251-7235-6-6

Muniz, F. T. L., Miranda, M. R., Morilla dos Santos, C., & Sasaki, J. M. (2016). The Scherrer equation and the dynamical theory of X-ray diffraction. *Acta Crystallographica Section A: Foundations and Advances*, *72*(3), 385-390.

Nettleton, J. A., Brouwer, I. A., Geleijnse, J. M., & Hornstra, G. (2017). Saturated Fat Consumption and Risk of Coronary Heart Disease and Ischemic Stroke: A Science Update. *Ann Nutr Metab*, *70*(1), 26-33. https://doi.org/10.1159/000455681

Patel, A. R., & Dewettinck, K. (2016). Edible oil structuring: an overview and recent updates. *Food Funct*, *7*(1), 20-29. https://doi.org/10.1039/c5fo01006c

Rabiei, M., Palevicius, A., Monshi, A., Nasiri, S., Vilkauskas, A., & Janusas, G. (2020). Comparing Methods for Calculating Nano Crystal Size of Natural Hydroxyapatite Using X-Ray Diffraction. *Nanomaterials (Basel)*, *10*(9). https://doi.org/10.3390/nano10091627

Rondou, K., De Witte, F., Rimaux, T., Dewinter, W., Dewettinck, K., Verwaeren, J., & Van Bockstaele, F. (2022). Multiscale analysis of monoglyceride oleogels during storage. *Journal of the American Oil Chemists' Society*, *99*(11), 1019-1031. https://doi.org/https://doi.org/10.1002/aocs.12645

Vereecken, J., Meeussen, W., Foubert, I., Lesaffer, A., Wouters, J., & Dewettinck, K. (2009). Comparing the crystallization and polymorphic behaviour of saturated and unsaturated monoglycerides. *Food Research International*, *42*, 1415–1425.

Verstringe, S., Danthine, S., Blecker, C., Depypere, F., & Dewettinck, K. (2013). Influence of monopalmitin on the isothermal crystallization mechanism of palm oil. Food Research International, 51(1), 344-353. https://doi.org/https://doi.org/10.1016/j.foodres.2012.12.034

Walstra, P., Kloek, W., & van Vliet, T. (2001). Fat Crystal Networks. In N. Garti, & K. Sato (Eds.), Crystallization Processes in Fats and Lipids (pp. 289-328). Marcel Dekker.

Watanabe, A. (1997). On the sub-α-form and the α-form in monoacylglycerols. *Journal of the American Oil Chemists' Society*, *74*(12), 1569-1573. https://doi.org/10.1007/s11746-997-0079-z

WHO. (2023, 17/07/2023). *WHO updates guidelines on fats and carbohydrates*. Retrieved 09 from https://www.who.int/news/item/17-07-2023-who-updates-guidelines-on-fats-and-carbohydrates#:~:text=Fat%20consumed%20by%20everyone%202,produced%20and%20ruminant%20animal%20sources.

6 Tables

Table 1. Onset temperature (T_{onset}), peak temperature (T_{peak}) and enthalpy of crystallization for monoglyceride oleogels MO-C18 and MO-C18/C16. Significant differences ($p<0.05$) between MO-C18 and MO-C18/C16 are indicated with letters a-b.

Peak	MO-C18			MO-C18/C16		
	T_{onset} (°C)	T_{peak} (°C)	Enthalpy (J/g)	T_{onset} (°C)	T_{peak} (°C)	Enthalpy (J/g)
1	57.6 ± 0.3[a]	55.5 ± 0.6[a]	9.4 ± 0.6[a]	52.2 ± 0.1[b]	50.9 ± 0.1[b]	12.0 ± 0.6[b]
2	38.8 ± 0.3[a]	37.8 ± 0.3[a]	2.2 ± 0.2[a]	16.7 ± 0.2[b]	15.7 ± 0.3[b]	1.2 ± 0.1[b]
3	28.5 ± 0.3	25.3 ± 0.5	0.2 ± 0.1	-	-	-

Table 2. Thickness of one lamella (d_{001}) and CNP thickness (L-CNP) of SR-MO-C18 and SR-MO-C18/C16.

Isothermal	**MO-C18**		**MO-C18/C16**	
temperature (°C)	d_{001} (Å)	L-CNP (nm)	d_{001} (Å)	L-CNP (nm)
10°C	49.6	362.0	50.1	330.3
20°C	49.6	356.2	50.9	315.5
25°C	49.6	364.6	51.0	333.0

7 Figures

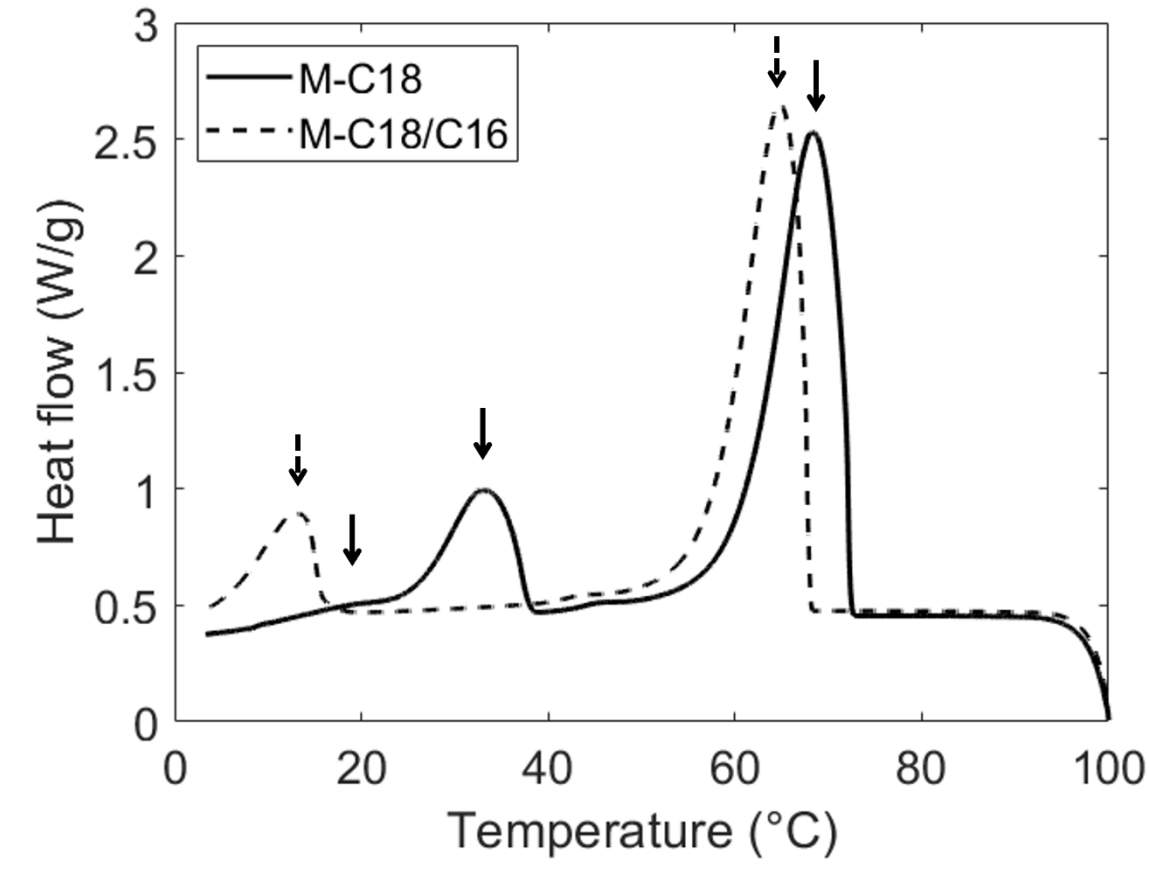

Figure 1. Crystallization curve of M-C18 and M-C18/C16 when cooled at 10°C/min.

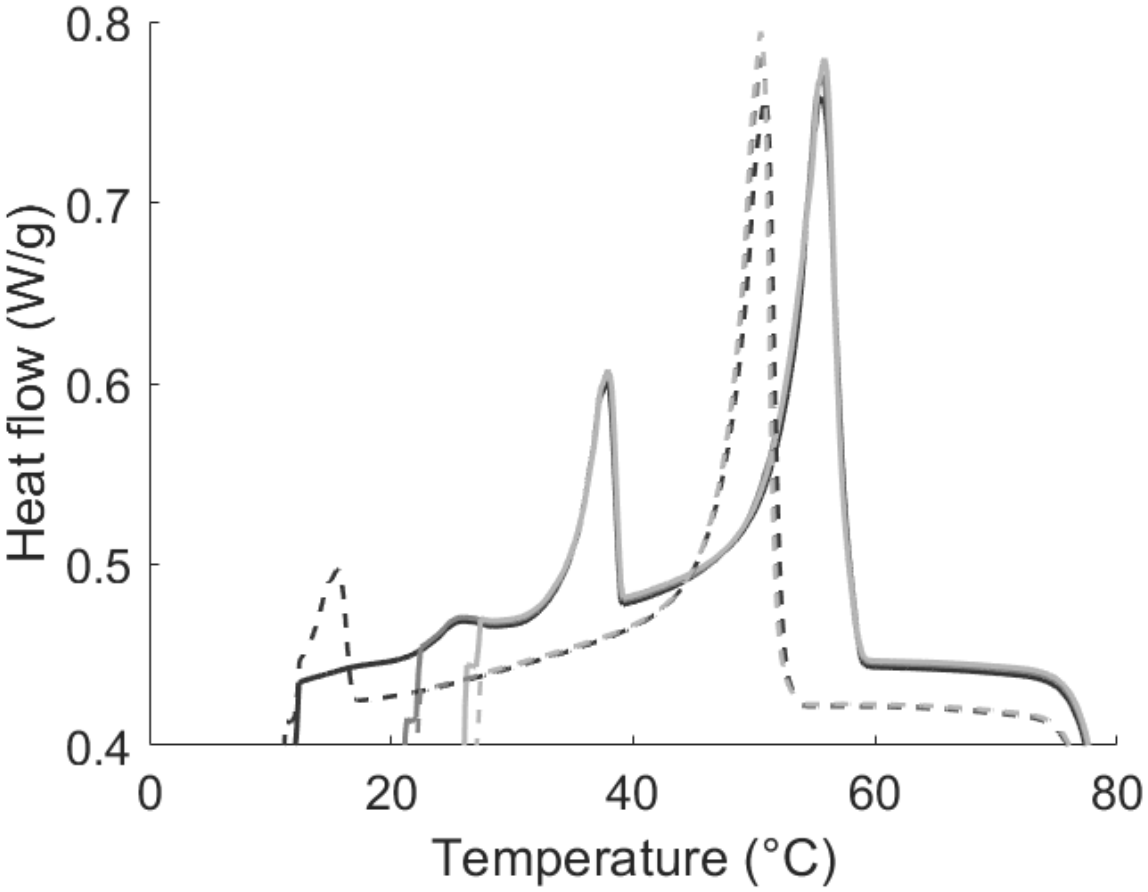

447

448 **Figure 2.** Crystallization curve of MO-C18 (full line) and MO-C18/C16 (dotted line) when cooled at
449 10°C/min till 10°C (black), 20°C (grey) or 25°C (light grey).

450

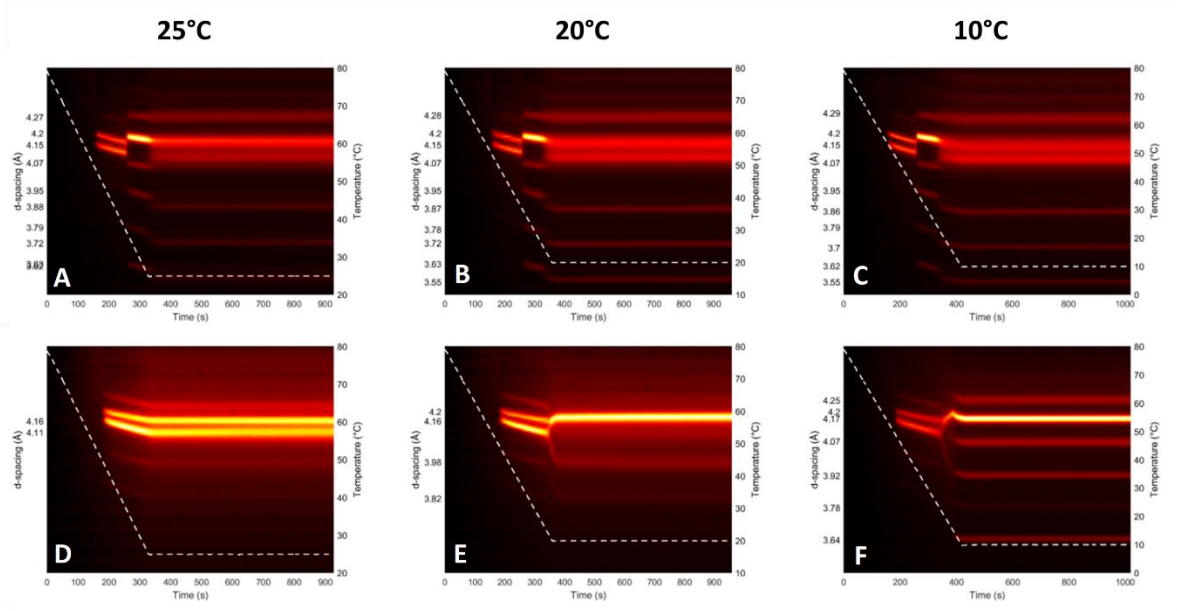

451 **Figure 3.** Heatmaps of SR-time-resolved WAXS of MO-C18 (A-C) and MO-C18/C16 (D-F) when cooled till
452 25°C, 20°C and 10°C at 10°C/min.

453

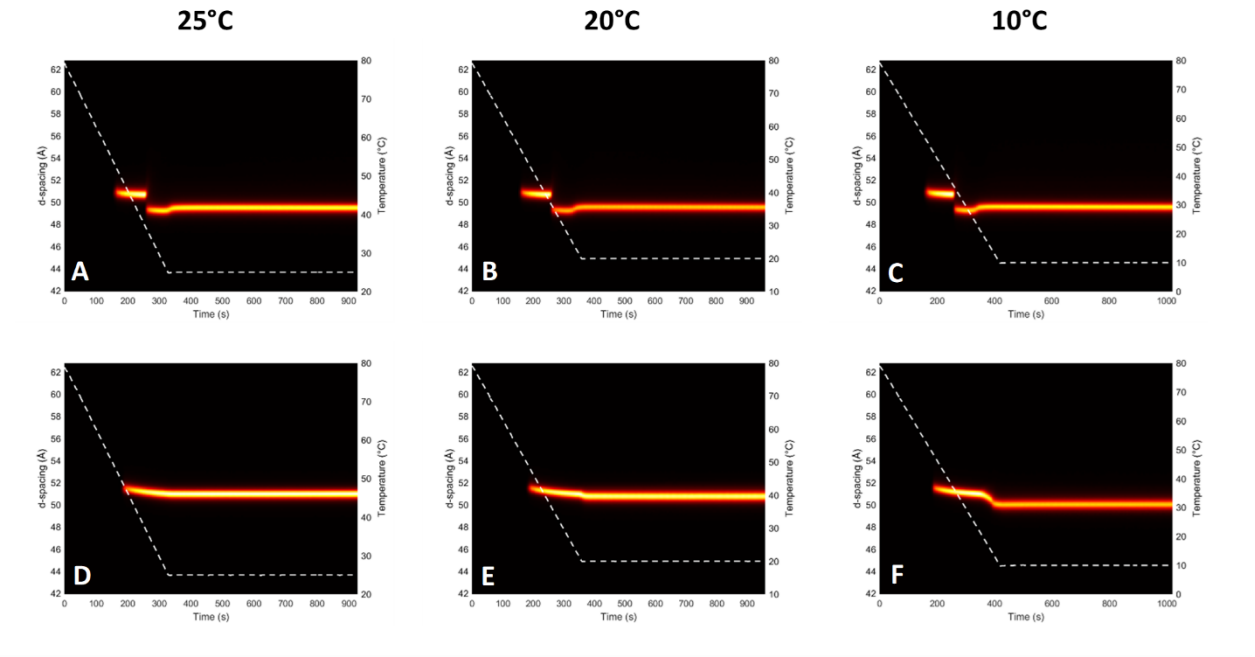

454 **Figure 4.** Heatmaps of SR-time-resolved SAXS of MO-C18 (A-C) and MO-C18/C16 (D-F) when cooled till
455 25°C, 20°C and 10°C at 10°C/min.

456

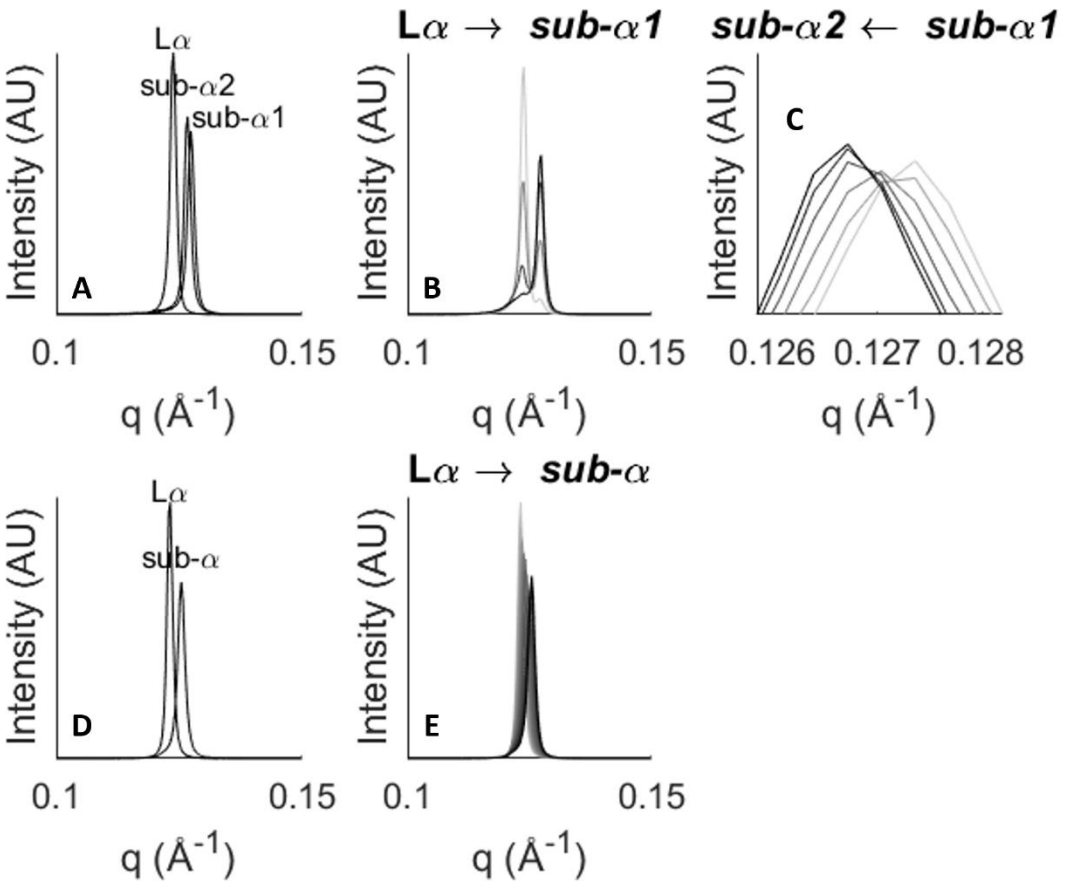

457 **Figure 5.** SR-SAXS profiles of the different polymorphs present during crystallization of MO-C18 (A) and
458 MO-C18/C16 (D) together with the SR-SAXS transitions (from light to dark grey) from Lα to sub-α1 (B)
459 and sub-α1 to sub-α2 (C) for MO-C18 and from Lα to sub-α (E) for MO-C18/C16 upon cooling at
460 10°C/min.

461

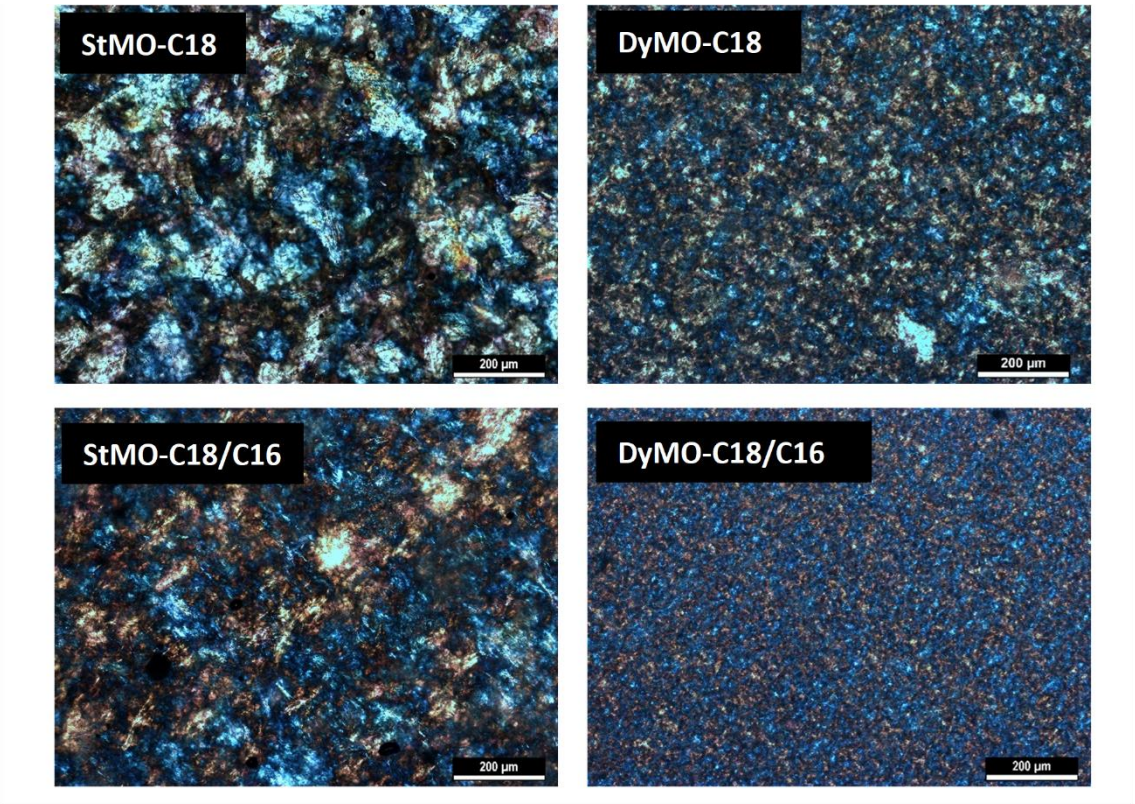

462 **Figure 6.** Polarized light microscopy images of statically crystallized (StMO) and dynamically crystallized
463 (DyMO) MO-C18 and MO-C18/C16. The scale bar is 200 µm.

464

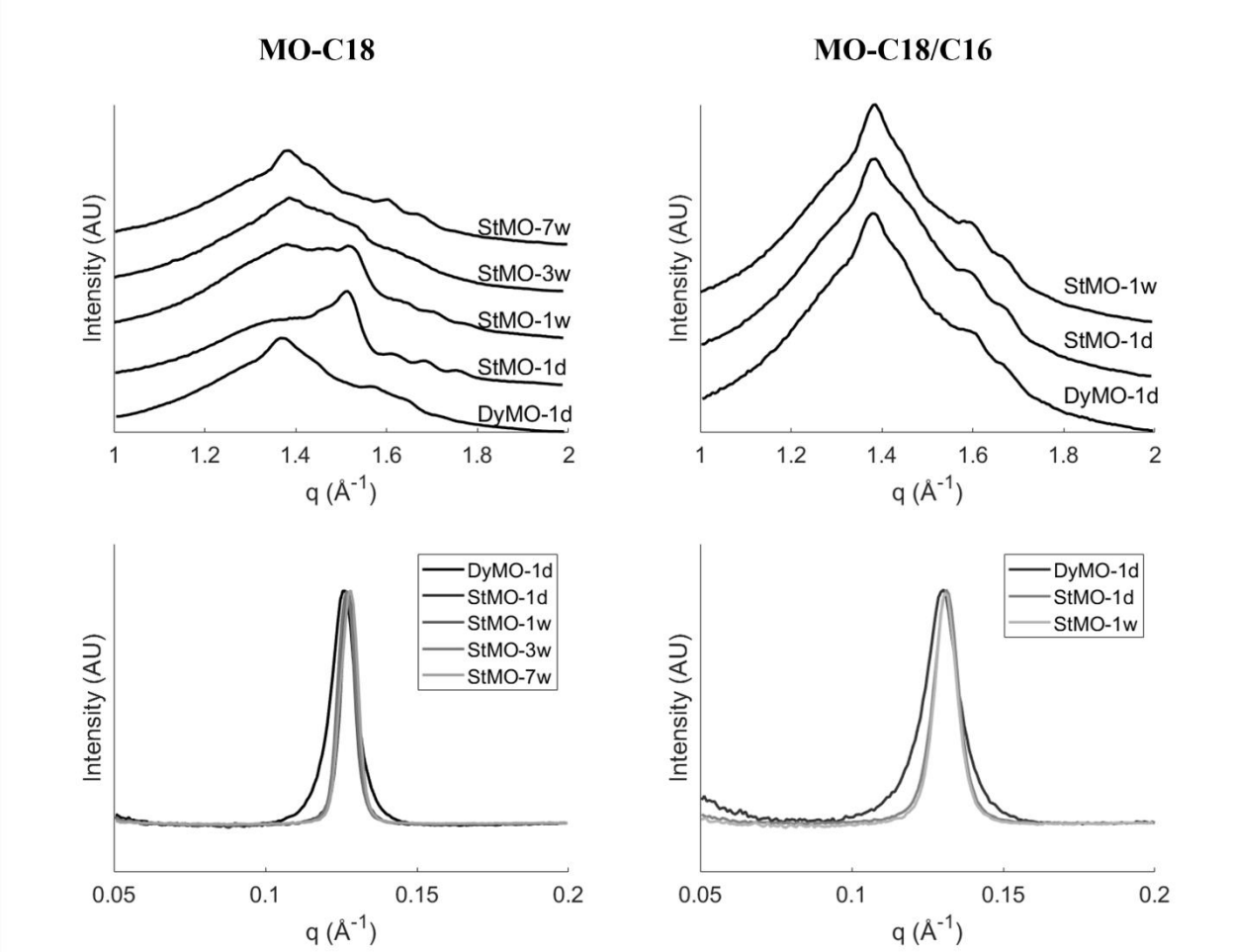

Figure 7. WAXS (top) and SAXS (bottom) profiles of statically (StMO) and dynamically (DyMO) crystallized MO-C18 and MO-C18/C16 as function of the storage time.

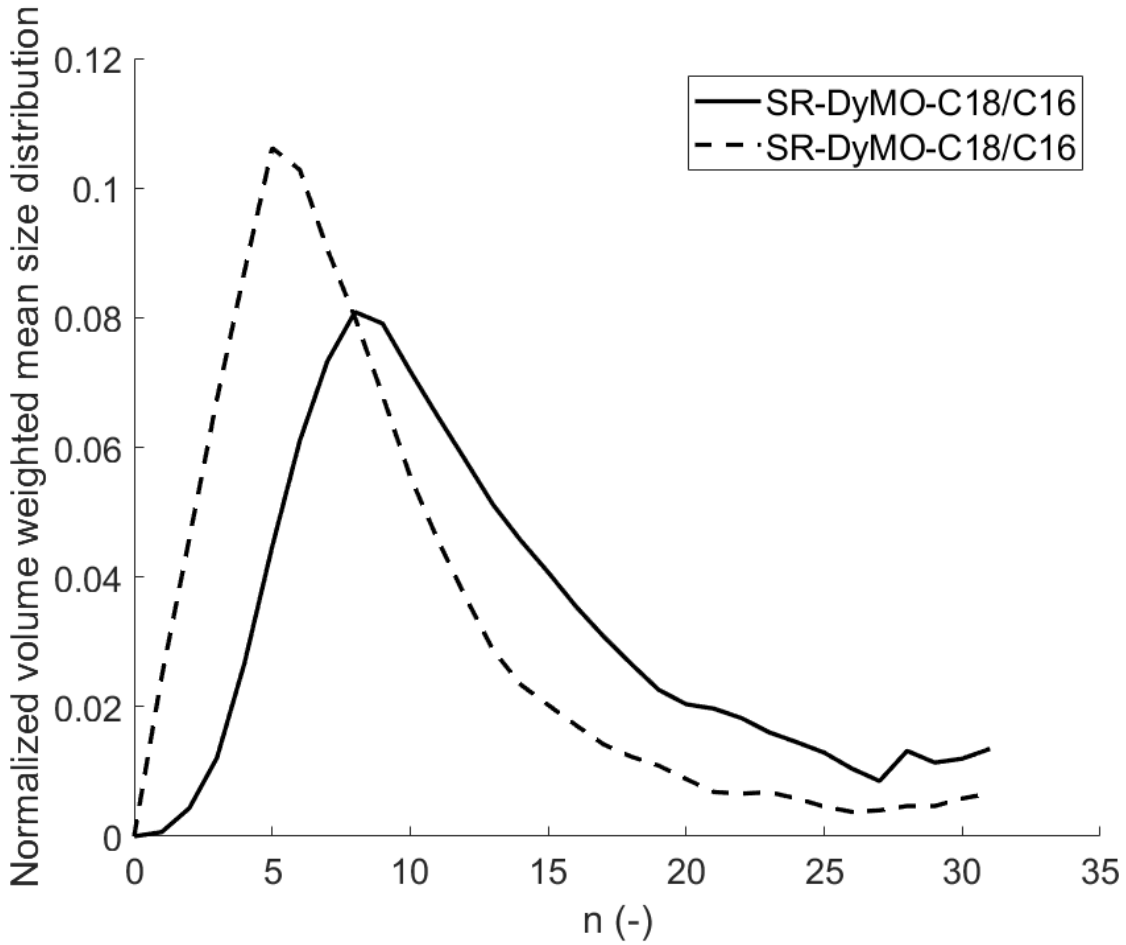

468 **Figure 8.** Normalized volume weighted distribution of SR-DyMO-C18 and SR-DyMO-C18/C16.

469

8 Supplementary data

Table S1. Onset and peak temperature of crystallization of the neat monoglycerides and the monoglyceride oleogels.

Peak	MO-C18			M-C18	MO-C18/C16			M-C18/C16
	10°C	20°C	25°C		10°C	20°C	25°C	
Onset temperature of crystallization								
1	57.6 ± 0.3	57.5 ± 0.2	57.4 ± 0.2	72.3 ± 0.1	52.2 ± 0.1	51.9 ± 0.1	51.71 ± 0.04	67.9 ± 0.2
2	38.8 ± 0.3	38.8 ± 0.3	38.8 ± 0.3	37.9 ± 0.2	16.7 ± 0.2	-	-	15.8 ± 0.1
3	28.5 ± 0.3	28.4 ± 0.4	-	21.1 ± 0.9	-	-	-	-
Peak temperature of crystallization								
1	55.5 ± 0.6	55.6 ± 0.2	55.7 ± 0.4	68.3 ± 0.6	50.9 ± 0.1	50.6 ± 0.1	50.58 ± 0.03	64.8 ± 0.5
2	37.8 ± 0.3	37.9 ± 0.4	37.9 ± 0.4	33.3 ± 0.4	15.6± 0.3	-	-	13.4 ± 0.2
3	25.3 ± 0.5	25.4 ± 0.6	-	17.8 ± 1.0	-	-	-	-